

LETTER • OPEN ACCESS

Diverging pond dissolved organic matter characteristics yield similar CO₂ flux potentials in a disturbed High Arctic landscape

To cite this article: J K Heslop *et al* 2021 *Environ. Res. Lett.* **16** 044016

View the [article online](#) for updates and enhancements.

ENVIRONMENTAL RESEARCH
LETTERS

LETTER

OPEN ACCESS

RECEIVED
18 December 2019REVISED
20 October 2020ACCEPTED FOR PUBLICATION
10 November 2020PUBLISHED
16 March 2021

Original content from
this work may be used
under the terms of the
[Creative Commons
Attribution 4.0 licence](#).

Any further distribution
of this work must
maintain attribution to
the author(s) and the title
of the work, journal
citation and DOI.

Diverging pond dissolved organic matter characteristics yield
similar CO₂ flux potentials in a disturbed High Arctic landscapeJ K Heslop^{1,4,*} , J K Y Hung¹ , H Tong² , M J Simpson², F M Chapman^{3,5}, N Roulet³, M J Lafrenière¹ 
and S F Lamoureux¹¹ Department of Geography and Planning, Queen's University, Kingston, Canada² Environmental NMR Centre and Department of Physical and Environmental Sciences, University of Toronto Scarborough, Toronto, Canada³ Department of Geography, McGill University, Montreal, Canada⁴ Current address: Section 3.7 Geomicrobiology, Helmholtz Centre Potsdam GFZ German Research Centre for Geosciences, Potsdam, Germany⁵ Current address: School of Geography and Earth Sciences, McMaster University, Hamilton, Canada

* Author to whom any correspondence should be addressed.

E-mail: jheslop@gfz-potsdam.de**Keywords:** carbon, permafrost, High Arctic, dissolved CO₂, pondsSupplementary material for this article is available [online](#)**Abstract**

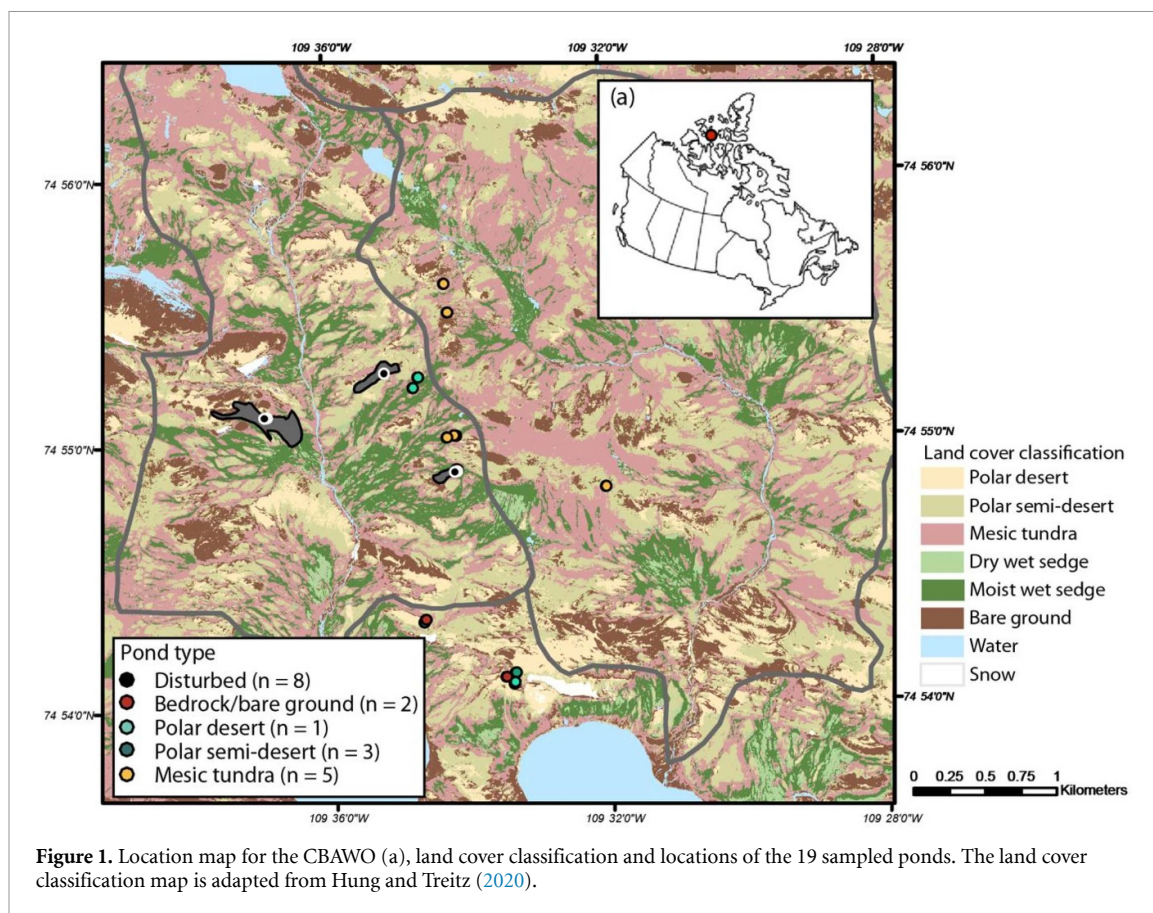
Climate warming and permafrost thaw have the potential to shift Arctic carbon (C) cycling dynamics so ponds, which represent over a quarter of northern circumpolar surface water area, may play a larger role in the mineralization of terrestrial C and emission of greenhouse gases (GHG). Here, we constrain how active layer detachments (ALDs) affect C cycling dynamics in High Arctic ponds ($n = 19$) through the examination of geochemistry, dissolved organic matter (DOM) characteristics, and dissolved GHG concentrations. Summer rainfall events were identified as the primary source of pond water over a 5 week period during the monitored thaw season. We observed two distinct geochemical and DOM composition groups in ponds surrounded by undisturbed, vegetated areas compared to ponds located within the geomorphologically-disturbed ALDs. DOM in undisturbed areas had characteristics suggesting allochthonous origin from modern vegetation. Ponds in the ALDs had lower mean dissolved organic carbon (DOC) concentrations than ponds within undisturbed landscapes, with DOM characterization suggesting greater proportions of autochthonous DOM. Observed differences in DOC concentrations and DOM composition between ponds located within the disturbed and undisturbed landscapes did not translate into significant differences in dissolved CO₂ concentrations among pond types. We conclude that our observed changes in DOM composition and characteristics in High Arctic ponds may not result in substantial increases in GHG flux as a result of continued Arctic warming.

1. Introduction

Lakes and ponds are common features in permafrost landscapes and have been identified as hotspots for the mineralization of terrestrial carbon (C) and its emission as greenhouse gases (GHG) to the atmosphere (Kuhn *et al* 2018). Under modern C cycling conditions, Arctic lakes and ponds have been shown to have varying GHG emission potentials. Some lakes, especially thermokarst (permafrost thaw) lakes, have been shown to have high GHG emissions (Walter *et al* 2006, Serikova *et al* 2019). However, many Arctic lakes are net sinks of CO₂ (Walter Anthony *et al* 2014,

Bouchard *et al* 2015). Small ponds (<1000 m²), representative of ~25% of northern circumpolar surface water area, currently play a negligible role in the mineralization of terrestrial-derived C and emissions of GHG (Polishchuk *et al* 2018, Bogard *et al* 2019). Continued climate warming and consequent permafrost thaw may shift these dynamics, with ponds potentially playing a larger role in future Arctic C cycling dynamics.

Permafrost thaw processes (e.g. active layer thickening, thermokarst, and thermo-erosion) are anticipated to release previously frozen, sequestered permafrost C (Schoor *et al* 2015). Permafrost thaw



events that result in mass movement of sediment (e.g. active layer detachment landslides and retrogressive thaw slumps) have increased in magnitude and frequency during recent decades (Lewkowicz and Way 2019), rapidly mobilizing large volumes of soil, altering landscape drainage dynamics, and mobilizing previously inaccessible soil organic matter (Turetsky *et al* 2020). The initiation rates of such thaw disturbance events are projected to continue increasing with future climate warming (Lewkowicz and Harris 2005, Lewkowicz and Way 2019). These events have been shown to alter geochemical and dissolved organic matter (DOM) characteristics when coupled with inland waters (Abbott *et al* 2014, Fouché *et al* 2017, Wang *et al* 2018); however, the impact and persistence of permafrost disturbances on GHG flux potentials from small Arctic ponds is not well understood or quantified.

Here, we examine pond geochemistry in combination with DOM characteristics and dissolved CO₂ concentrations to improve our understanding of the impact of active layer detachments (ALDs) on C cycling dynamics in High Arctic ponds. This research was conducted at the Cape Bounty Arctic Watershed Observatory (CBAWO), Melville Island, Nunavut, in the Canadian High Arctic (74°54'N, 109°35'W; figure 1(a)). The CBAWO is underlain by continuous permafrost and is located in an understudied region for published Arctic research (Metcalf *et al* 2018). We hypothesized that ponds located within the ALDs

would contain more DOC with more biolabile DOM characteristics and greater GHG flux potentials, indicated by higher dissolved GHG concentrations, compared to ponds located in undisturbed sites, where we hypothesized surrounding modern vegetation type would be the dominant influence on DOM composition.

2. Methods

2.1. Study site and sample collection

Nineteen ponds were selected for monitoring over a 6 week period during the late thaw season at the CBAWO (16 July–12 August 2018; figure 1). Each sample date was classified by antecedent meteorological conditions (temperature and rainfall) during the week prior compared to the longer-term (2003–2018) July–August means (cold wet, cold dry, warm wet, warm dry; figure S1 (available online at stacks.iop.org/ERL/16/044016/mmedia); Beel *et al* 2018). Each pond was further classified according to its surrounding vegetation class (bedrock/bare ground, mesic tundra, polar desert, polar semi-desert; Hung and Treitz 2020) and disturbance regime (table S1; figure 2). Ponds in locations geomorphologically affected by ALDs were classified as disturbed (figures 2(a) and (b)); ponds in locations experiencing active layer thickening but that were not affected by ALDs were classified as undisturbed (figures 2(c)–(f); Beel *et al* 2020). The active layer detachments

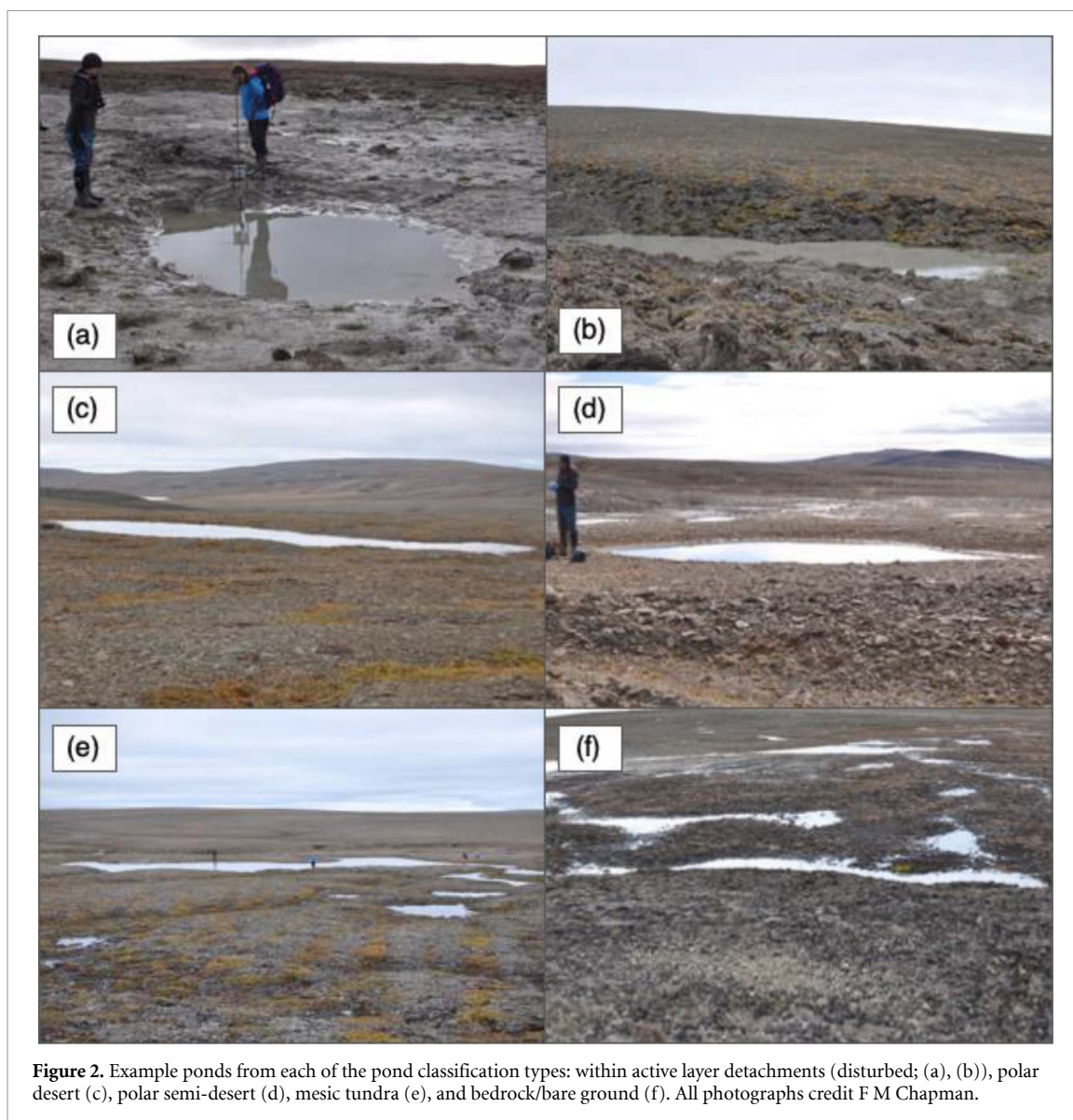


Figure 2. Example ponds from each of the pond classification types: within active layer detachments (disturbed; (a), (b)), polar desert (c), polar semi-desert (d), mesic tundra (e), and bedrock/bare ground (f). All photographs credit F M Chapman.

in which our disturbed sampled ponds were located occurred in 2007–2008 (Lamoureux and Lafrenière 2018).

For each pond site, we noted whether standing water was present or absent. When water was present, pH, EC, and relative turbidity were measured on unfiltered samples at the in-field laboratory using a benchtop pH and EC probe (Orion Star A215) and portable turbidity meter (LaMotte 2020wi). Water filtration was conducted within 1–5 h of sampling using methods described in Lafrenière *et al* (2017). All samples were kept cool (<8 °C) and in the dark in the field (2–3 weeks after collection due to remote field logistics), then were transported to Queen’s University and refrigerated (4 °C) until further analyses (3–7 weeks after collection).

2.2. Hydrochemistry

Stable isotope values of hydrogen (δD) and oxygen ($\delta^{18}O$) were determined from 0.22 μm filtered water samples using a Los Gatos Research laser absorption

liquid water isotope analyzer; we report δD (analytical uncertainty $\pm 0.8\text{‰}$) and $\delta^{18}O$ (analytical uncertainty $\pm 0.2\text{‰}$) as deviations in per mil from the Vienna Standard Mean Ocean Water composition (‰ VSMOW). Concentrations of dissolved organic carbon (DOC) and total dissolved nitrogen (TDN) were measured on 0.7 μm filtered water samples using a Shimadzu TOC-L with TMN-L. Concentrations of major ions (Br^- , Ca^{2+} , Cl^- , F^- , K^+ , Li^+ , Mg^{2+} , Na^+ , NH_4^+ , NO_2^- , NO_3^- , PO_4^{3-} , SO_4^{2-}) and organic acids (acetate, butyrate, formate, oxalate) were measured by liquid ion chromatography on 0.22 μm filtered water samples using a Dionex ICS-5000 equipped with an AERS 500 suppressor and an AS18 analytical column for anions and CERS 500 suppressor and C12A analytical column for cations. The instrument detection limits were 0.01 $mg\ l^{-1}$, and analytical uncertainties were between 5 and 20 $\mu g\ l^{-1}$.

2.3. DOM spectroscopy

Optical properties of chromophoric dissolved organic matter (CDOM) and fluorescent dissolved organic

matter (FDOM) were determined using a Horiba Aqualog. In these analyses, DOM is operationally defined as $<0.7 \mu\text{m}$. Data collection parameters and equations used for CDOM and FDOM calculations are presented in the Supplementary Information. CDOM data were used to calculate: (1) specific UV absorbance at 254 nm (SUVA_{254} ; $1 \text{ mg C}^{-1} \text{ m}^{-1}$), a parameter that is commonly used as an index of DOM aromaticity (Weishaar *et al* 2003); (2) spectral slopes between 275–295 nm ($S_{275-295}$) and 350–400 nm ($S_{350-400}$); and (3) slope ratio (S_R ; $S_{275-295}:S_{350-400}$), which has been shown to correlate with average DOM molecular weight (Helms *et al* 2008). We also report absorption coefficients in Napierian units at wavelengths of 254 nm (α_{254}) and 350 nm (α_{350}), which have been shown to correlate with allochthonous-dominated DOM in riverine systems (Spencer *et al* 2012). Further, α_{350} has been previously shown to strongly correlate with lignin phenol concentrations (Spencer *et al* 2010), which are indicative of terrestrially-derived vascular plant material in DOM (Mann *et al* 2016). Using the FDOM data, we calculated: (1) fluorescence index (FI), a measure of the relative contribution of terrestrial and microbial DOM sources (Cory *et al* 2010); (2) humification index (HIX), an indicator of the degree of DOM humification (Ohno, 2002); (3) freshness index ($\beta:\alpha$), an indicator of recently-produced DOM (Wilson and Xenopoulos 2009); (4) the relative fluorescence index (RFE), and indicator of algal versus non-algal DOM (Downing *et al* 2009); and (5) the biological index (BIX), an indicator of autochthonous-origin DOM (Huguet *et al* 2009).

2.4. Nuclear magnetic resonance (NMR) spectroscopy

We collected and immediately froze additional water samples at biweekly intervals from a subset of three ponds (two ponds located within active later detachments and one pond located in an undisturbed mesic tundra area; table S1) for solution-state NMR analyses. Following the method of Wang *et al* (2018; see supplementary information), we collected and processed 2048 scans for each one-dimensional ^1H NMR spectrum. For the purposes of this study, we integrated the one-dimensional ^1H NMR spectra into four regions (figure S5): (1) materials derived from linear terpenoids (MDLT; 0.6–1.6 ppm); (2) carboxyl-rich alicyclic molecules (CRAM; 1.6–3.2 ppm); (3) carbohydrates and peptides (3.2–4.5 ppm); and (4) aromatics and phenolics (6.5–8.4 ppm). Results are presented as the percent relative abundance of the total ^1H signal.

2.5. Dissolved gas concentrations

Dissolved gas samples were collected from a subset of 13 ponds (table S1) simultaneously with the collection of water samples for analyses outlined prior. Water samples from the ponds were injected

into prepared serum vials then equilibrated with the headspace. Headspace CO_2 and CH_4 concentrations were measured on a Perkin Elmer Clarus 500 Gas Chromatograph. Dissolved gas concentrations in the water were calculated from headspace gas concentrations using Henry's Law and are reported in mg l^{-1} . For the purposes of this study, we interpret CO_2 flux potential as the potential diffusive flux from ponds to the atmosphere based on dissolved CO_2 concentrations in ponds versus atmospheric CO_2 concentration (Kling *et al* 1992). Dissolved CO_2 atmospheric equilibrium was calculated using Henry's Law and the mean pond water temperature for each sample date. We acknowledge that additional temporally-varying physical (e.g. wind speed and boundary layer thickness) and biological (e.g. rates of photosynthesis and heterotrophic respiration) factors that were not accounted for in our study affect the actual diffusive CO_2 flux from these ponds. Therefore, we refer to our dissolved CO_2 concentrations as being representative of CO_2 flux potentials.

2.6. Statistical analyses

All statistical analyses were conducted using MATLAB R2016a software. Pearson's linear correlation coefficients were calculated between all variables (table S3). For each variable, n -way analyses of variance were conducted among observations: (1) in ALD (disturbed) versus intact (undisturbed) land surfaces; (2) in each surrounding vegetation class; and (3) from each weekly antecedent meteorological classification (table S4). For variables where statistically significant ($p < 0.05$) differences among groups were detected, we conducted two sample t -tests (tables S5 and S6) and ran a principal component analysis to identify potential groupings in variables and observations (table S7, figure S3). We utilize previously published data from proximal ponds in the same watershed collected in 2015 ($n = 6$ observations; Wang *et al* 2018) and 2016 ($n = 12$ observations, Thiel 2018) in our statistical analyses (table S2). With the exception of pond area and dissolved gas concentrations, the same data were collected for all observations using the same methods in each year.

3. Results

3.1. Hydrochemistry

During our first sample date (16 July), six pond sites contained no standing water; by 06 August, all pond sites had water present. Stable water isotope values showed less variation among ponds as the sampling season progressed. No statistically significant differences were identified among land cover groups or meteorological condition groups (figure 3). Concentrations of DOC ranged between 0.87 and 15.8 mg l^{-1} and were consistently higher in ponds surrounded by undisturbed vegetated areas compared to ponds located within the ALDs (figure 4(a)).

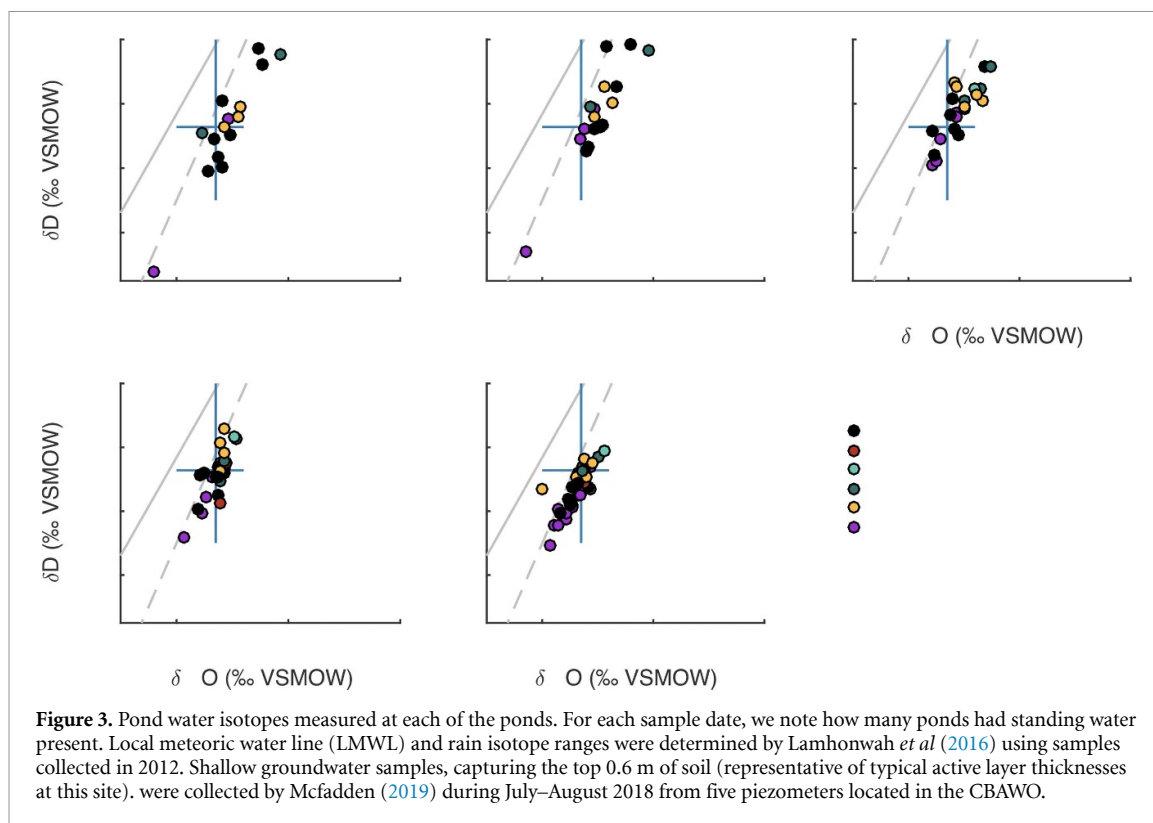


Figure 3. Pond water isotopes measured at each of the ponds. For each sample date, we note how many ponds had standing water present. Local meteoric water line (LMWL) and rain isotope ranges were determined by Lamhonwah *et al* (2016) using samples collected in 2012. Shallow groundwater samples, capturing the top 0.6 m of soil (representative of typical active layer thicknesses at this site), were collected by Mcfadden (2019) during July–August 2018 from five piezometers located in the CBAWO.

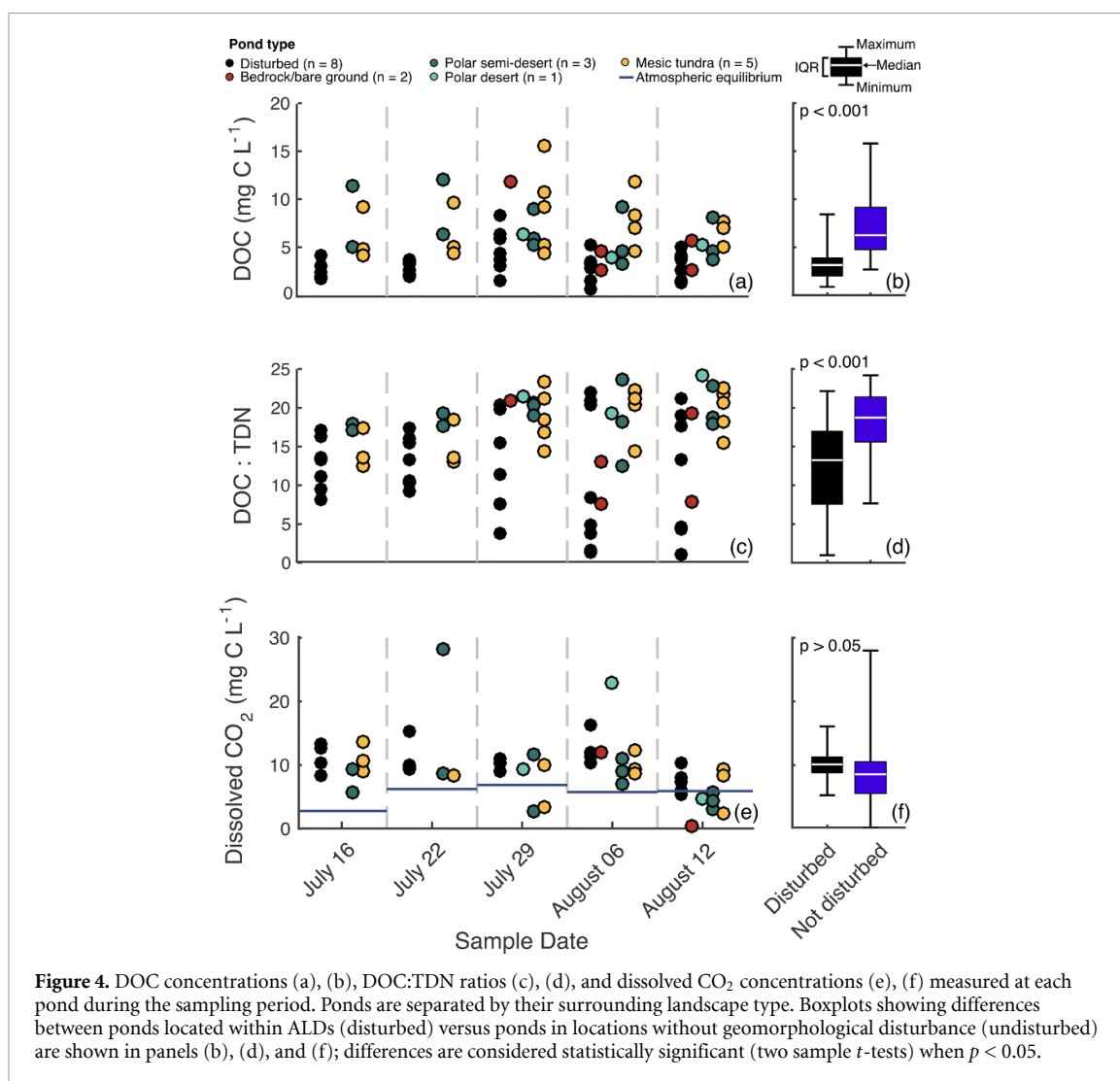
Mean DOC concentrations were highest in samples preceded by warm and wet antecedent conditions. TDN concentrations ranged from 0.11 to 2.80 mg l⁻¹ (figure S7) and ratios of DOC:TDN ranged from 0.98 to 24.2 (figure 4(b)). While there were no significant differences in TDN concentrations, ponds located in ALDs had lower DOC:TDN ratios compared to ponds in undisturbed areas. Disturbed ponds had higher concentrations of in K⁺, Na⁺, NH₄⁺, and formate compared to ponds in undisturbed areas; ponds in undisturbed areas had higher concentrations of Ca²⁺, F⁻, and acetate compared to ponds in disturbed areas (figures S8–S12).

3.2. DOM spectroscopy

Optical properties indicate that ponds in undisturbed areas had higher proportions of allochthonous DOM compared to ponds in ALDs. Allochthonous DOM, in particular vascular plant material (α_{350} ; figure S13(b)), increased during the sampling period in the undisturbed ponds. S_R values ranged from 0.26 to 1.17 and were consistently higher in ponds located in the ALDs (figure S16(a)). Ponds located in the polar semi-desert and mesic tundra had the lowest S_R values. $SUVA_{254}$ values ranged from 2.15 to 17.23 l mg C⁻¹ m⁻¹, were highest in the disturbed and bedrock/bare ground ponds, and lowest in the polar semi-desert and mesic tundra ponds (figure S16(b)). High $SUVA_{254}$ values may indicate the possible presence of high iron (Fe) concentrations in our ponds (Poulin *et al* 2014), fine particulates that passed through our 0.7 micron filters (Weishaar *et al*

2003, Massicotte *et al* 2017), and/or some contamination that is not able to be constrained or corrected by other measurements. We did not measure Fe concentrations in this study to correct our optical data for the effects of Fe, but data collected from a subset of these ponds at the CBAWO in 2019 suggest dissolved Fe concentrations are too low to significantly interfere with optical DOM measurements (32–130 ppb; Lafrenière, unpublished data). We did not observe any particles, colloids, or precipitation in our samples prior to our measurements, indicating particulates were successfully removed during sample filtration. Further, in terrestrial aquatic ecosystems such as the ponds at the CBAWO, fine particles that pass through a 0.7 micron filter have been shown to not significantly affect the DOM absorption signal (Massicotte *et al* 2017). Neither $SUVA_{254}$ nor S_R values varied among meteorological periods.

BIX values ranged from 0.53 to 1.00, FI values ranged from 1.21 to 1.66, and $\beta:\alpha$ values ranged from 0.52 to 0.97. Strong correlation between BIX and $\beta:\alpha$ values (Pearson $r = 0.98$; table S3) suggest these parameters convey the same information about pond DOM. BIX, FI and $\beta:\alpha$ values were highest in the disturbed ponds and lowest in the polar semi-desert and mesic tundra ponds (figures S13 and S14). HIX values ranged from 0.52 to 1.1, were lowest in the disturbed and polar desert ponds, and highest in the polar semi-desert and mesic tundra ponds (figure S14(b)). RFE values ranged from 0.0145 to 0.0249 and were lower in the bedrock/bare ground and polar desert



ponds than in the polar semi-desert and mesic tundra ponds (figure S14(c)). None of these FDOM parameters significantly differed among the antecedent meteorological periods.

3.3. NMR DOM characterization

CRAM ($37 \pm 3\%$ relative abundance) and MDLT ($32 \pm 3\%$ relative abundance) were the most abundant compound classes in our NMR analyses (figure S4). Higher relative abundance of MDLT corresponded with higher relative abundance of CRAM and lower relative abundances of carbohydrates, peptides, and aromatic compounds (table S3). Higher relative abundance of carbohydrates and peptides also corresponded with lower relative abundance of CRAM. Relative abundance of compound classes did not significantly differ between disturbed and undisturbed locations or among the antecedent meteorological periods (table S4).

3.4. Dissolved gas concentrations

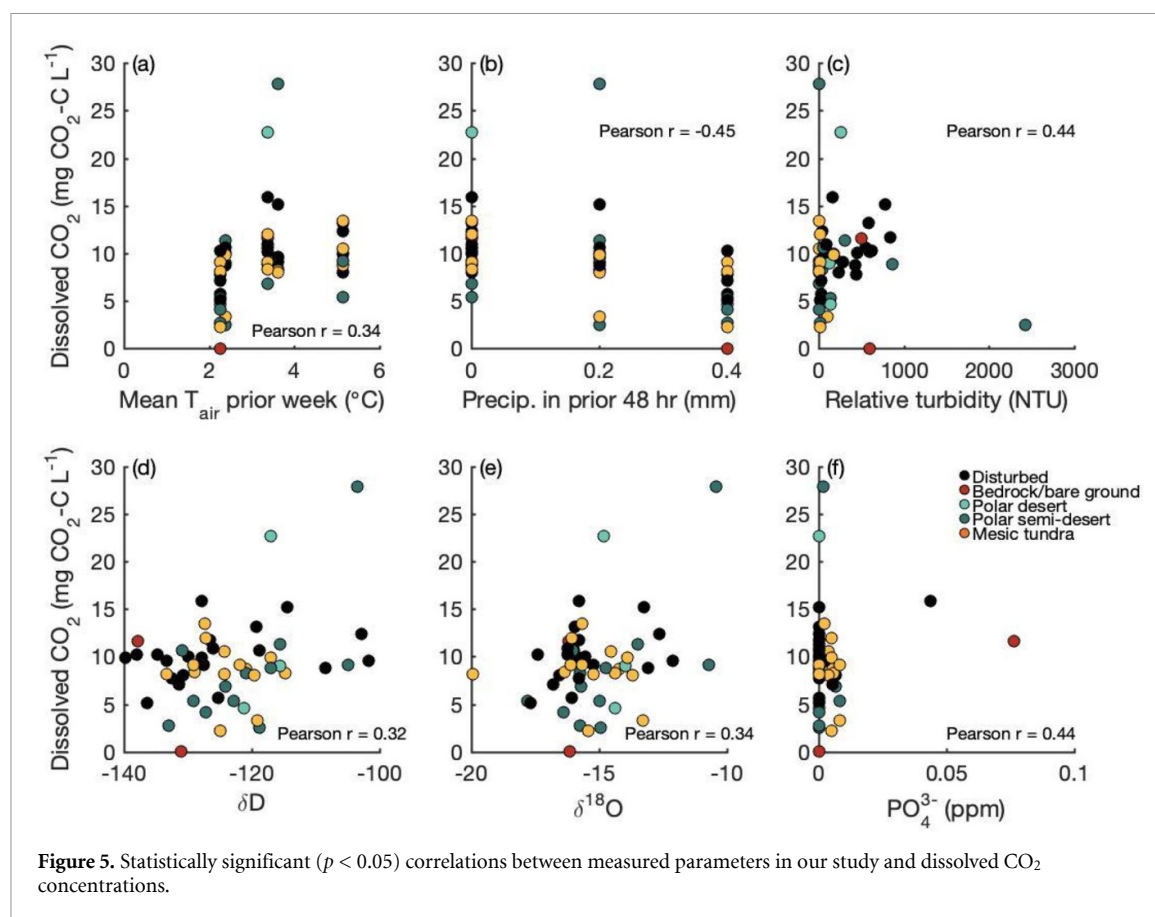
Dissolved CO₂ concentrations ranged from 0 to 27.8 mg C-CO₂ l⁻¹ (mean \pm SD 9.2 ± 4.6 mg C-CO₂ l⁻¹; figure 4(c)). While there were no significant

differences among pond types (table S4), sample dates with preceding meteorological conditions classified as cold and dry had significantly lower dissolved CO₂ concentrations (table S6). Dissolved CO₂ concentrations in ponds correlated with: mean atmospheric temperatures during the preceding week (Pearson $r = 0.34$); precipitation during the preceding 48 h ($r = -0.45$); δ D ($r = 0.32$) and δ^{18} O ($r = 0.34$); PO₄³⁻ concentrations ($r = 0.44$); and relative turbidity ($r = 0.44$; figure 5). We note that dissolved CO₂ concentrations did not significantly correlate with DOC concentrations or any DOM characteristics measured in this study (table S3). Dissolved CH₄ was below the detection limit (0.1 ppm) for all samples.

4. Discussion

4.1. Land cover controls pond geochemistry and DOM

Spatial variability in pond geochemistry and DOM characteristics was largely explained by differences in surrounding land cover type. The majority of



DOM in all ponds was allochthonous, fresh (indicated by high $\beta:\alpha$ values), and terrestrially-derived (FI values < 1.66 and BIX values < 1.0). We observed greater proportions of allochthonous DOM (indicated by higher α_{254} , α_{350} , and RFE values) in the undisturbed ponds. This DOM had higher average molecular weight (indicated by lower S_R values) and was more influenced by humic vascular plant material (indicated by higher α_{350} and HIX values) than DOM in ponds located within the ALDs. Ponds surrounded by land cover types with more above-ground biomass (polar semi-desert and mesic tundra; Hung and Treitz 2020) had higher DOC concentrations. Correlations between watershed above-ground biomass and terrestrial DOC export and production in surface runoff have also been found in Alaskan Arctic tundra (Judd and Kling 2002). This suggests modern vegetation is a major source of pond DOM in this High Arctic environment.

Ponds located within ALDs had greater proportions of autochthonous DOM (indicated by higher BIX and FI values) characterized by lower average molecular weight (higher S_R values) and greater aromatic content (higher SUVA_{254} values) than ponds in undisturbed areas. These findings correspond with complimentary work in stream headwaters at the CBAWO, which found increasing degrees of disturbance led to decreasing average molecular weight and humification (Fouché *et al* 2017). While it is

important to note BIX values in our study indicate the majority of DOM in all our ponds is allochthonous, the higher BIX and FI values in ponds located within ALDs is suggestive of greater primary productivity relative to the undisturbed ponds. We did not examine the sources of autochthonous DOM at the CBAWO, but data from other sites suggest benthic algae may be responsible for over 90% of primary productivity in shallow arctic lakes and ponds (Cazzanelli *et al* 2012). Combined, this suggests that: (a) C at disturbed sites is more bioavailable than C at undisturbed sites, potentially due to ponds in the ALDs sourcing a greater proportion of DOM from thawed permafrost OM; and/or (b) dissolved nutrient input from thawing soils stimulates increased primary productivity in ponds located within ALDs (Wauthy *et al* 2020).

It is important to note that ponds located in ALDs had consistently lower mean DOC concentrations than ponds located in undisturbed, vegetated sites (figure 4(a)). Lower DOC concentrations following permafrost disturbance were also found in the Peel Plateau, Canada (Littlefair *et al* 2017) and at the CBAWO in headwater streams (Fouché *et al* 2017, Beel *et al* 2020). However, this is the opposite of several other studies examining Arctic freshwaters, which found permafrost disturbance increases terrestrial C input and DOC export (Abbott *et al* 2014, Wauthy *et al* 2018). Lower mean DOC concentrations

in ponds within ALDs may partially be a function of underlying permafrost type at the CBAWO, which is less organic-rich ($\sim 1.5\%$ OC; figure S20) than permafrost underlying regions of Alaska and Siberia ($\sim 2.6\%$ OC; Strauss *et al* 2017) where several studies find increased DOC export following disturbance (Vonk *et al* 2013, Abbott *et al* 2014). Lower DOC concentrations in the ponds inside ALDs at the CBAWO may also be due to preferential sorption of higher molecular weight DOM to mineral soils (Kalbitz *et al* 2005) and/or a reduction in potential DOC inputs from surrounding vegetation into ponds.

Our results suggest disturbance of permafrost landscapes that results in mass sediment movement, such as ALDs, will likely decrease allochthonous DOC export to inland waters in this High Arctic region as it continues to warm. The decreased terrestrial DOC export to ponds at ALD sites at the CBAWO is important to consider in future C cycling models, given the current assumption is that rapid thaw disturbance events will increase C processing and export (Turetsky *et al* 2020). We propose additional research is necessary to determine what permafrost and/or landscape characteristics determine if disturbance events will increase (Abbott *et al* 2014, Wauthy *et al* 2018, Turetsky *et al* 2020) or decrease (this study; Littlefair *et al* 2017, Beel *et al* 2020) terrestrial C export to inland waters (Tank *et al* 2020).

4.2. Dissolved CO₂ concentrations influenced by physical factors

Ponds at both disturbed and undisturbed sites had similar dissolved CO₂ concentrations, indicating that they have similar GHG flux potentials. This suggests ALD events do not lead to long-term higher GHG fluxes from ponds in this landscape. Dissolved CO₂ concentrations in ponds did not spatially vary across land surfaces, despite differences in DOC concentrations and DOM composition. Freshwater systems located in the same watershed with similar dissolved CO₂ concentrations but dissimilar DOM characteristics have also been observed in the Canadian High Arctic near Lake Hazen, although this study attributed the lack of significant differences to high variability among observations (Emmertson *et al* 2016). At the CBAWO, ponds surrounded by undisturbed vegetation had, on average, three times higher DOC concentrations compared to ponds within the ALDs. This suggests that ponds located within the ALDs contain more biolabile DOM, potentially sourced from thawing permafrost (Mann *et al* 2014, Spencer *et al* 2015, Vonk *et al* 2015). Although DOC biodegradability was not directly measured in this study, higher indicators of autochthonous DOM (higher BIX, FI, and $\beta:\alpha$ values) in the ponds located in ALDs support that there are potentially higher biological C degradation rates.

Conversely, DOM exported to ponds located in undisturbed areas may be more modern and stable,

resulting in less mineralization to CO₂ (Textor *et al* 2019). While C biolability generally decreases with C age (Douglas *et al* 2020), preservation of OM in frozen permafrost can potentially lead to pre-aged permafrost OM being as or more biolabile than modern vegetation. Further, polyphenolic compounds from vascular plants can have an inhibitory effect on microbial carbon mineralization (Mann *et al* 2014, Kellerman *et al* 2015). However, one-dimensional ¹H NMR spectra results suggest aromatic and phenolic compounds are in low abundance (mean 2% relative abundance) at the CBAWO (figure S4); therefore, there may not be a strong inhibitory effect from these compounds at this site. The NMR spectra also show that the DOM in the undisturbed ponds have higher relative abundance of biolabile carbohydrate and peptide compounds (mean 17% relative abundance) than the disturbed ponds (mean 6% relative abundance). This suggests, at the CBAWO, DOM sourced from vegetation has high substrate potential to be biologically processed into GHG.

Our results show dissolved CO₂ concentrations in High Arctic ponds are controlled more by physical (temperature and precipitation) than geochemical (DOC concentrations and DOM characteristics) factors. We did not measure the relative influence of biological factors such as photosynthesis versus heterotrophic respiration rates. Positive correlation of dissolved CO₂ concentrations with antecedent rainfall and pond relative turbidity also suggest a portion of the CO₂ originates from surrounding soils. Dissolved CO₂ can originate from non-biological sources such as dissolution from atmospheric or diffusion (Laurion *et al* 2010), photodegradation (Rutledge *et al* 2010), and/or production of CO₂ from the dissociation of inorganic carbonates (Zolkos *et al* 2018). The CBAWO is overlain by carbonate-rich glacial till (Edlund 1993), and active layer soil profiles indicate the presence of inorganic C (IC) in both ALDs (mean \pm SD $0.11 \pm 0.16\%$) and undisturbed regions (mean \pm SD $0.06 \pm 0.11\%$ IC; figure S20). Positive correlation of rainfall in the prior 48 h with concentrations of several major ions (table S3) indicates water from rainfall events interact with deeper soils (exposed at the surface by disturbances and/or thawed at depth; Lewis *et al* 2012, Lamhonwah *et al* 2016, Toohey *et al* 2016) before entering ponds. Therefore, a portion of the dissolved CO₂ measured in our study may be non-biological in origin (e.g. originate from carbonates).

4.3. Potential changes with climate warming

Our spatially variable High Arctic ponds received increasingly similar water sources during the late-thaw season, despite their differing geochemical and DOM characteristics. By the end of the monitoring period, stable water isotope values in all ponds and in the shallow groundwater converged (figure 3). Snow is rapidly exhausted in this environment by

late June, with snowmelt runoff occurring over largely frozen landscapes (Favaro and Lamoureaux 2015), and groundwater is not a major component of the water budget due to the underlying continuous permafrost. Therefore, the water in all ponds was likely sourced from late summer rainfall (surface and sub-surface runoff responses; figures 3 and S17). Global climate models consistently predict increases in the magnitude and frequency of summer rainfall across the Arctic, with current model projections suggesting that rainfall will be dominant form of Arctic precipitation by the end of this century (Bintanja and Andry 2017). Given that the 2018 thaw season was the second wettest thaw season (68.6 mm precipitation in June–August) on record at the CBAWO (figure S1(b)), results from this study may be representative of pond characteristics under projected rainfall-dominated High Arctic climates.

Our results suggest, under these conditions, rainwater will be the dominant water source for small ponds during the thaw season (figure S17). Even though the source of pond water is homogenous across the landscape, DOC concentrations and DOM characteristics diverge depending on the characteristics of the surrounding landscape (Tank *et al* 2020). Rainfall events have been previously identified as important to replenishing DOM in peatlands (Pickard *et al* 2017) and coastal Arctic systems (Coch *et al* 2018). Further, prior research at the CBAWO suggests non-nival solute export (Lamhonwah *et al* 2016) and C export (Beel *et al* 2020) into streams are closely tied to the magnitude and frequency of rainfall events. Differences in pond geochemistry and DOM characteristics with different surrounding land cover classes observed in this study support that DOM export from the surrounding landscape, including during rainfall events, plays an important role in determining DOM concentrations and characteristics in ponds at the CBAWO.

In undisturbed land surfaces, ponds in vegetation classes with more above-ground biomass (polar semi-desert and mesic tundra) had higher mean DOC concentrations than ponds in the remaining vegetation classes. This highlights the importance of projecting vegetation cover changes in the High Arctic to predict subsequent changes in terrestrial C export to inland waters. Remote sensing data from 1985 to 2015 at the CBAWO indicate an overall greening trend, especially in mesic tundra ($+1.3\% \text{ yr}^{-1}$ Normalized Difference Vegetation Index; NDVI) and polar semi-desert ($+0.82\% \text{ yr}^{-1}$ NDVI) locations (Edwards and Treitz 2018). If this greening trend continues, results from our study suggest modern terrestrial C export into ponds will increase due to an increase above-ground biomass. Studies from Alaska and Siberia suggest this modern vegetation-derived DOM is bio-labile (O'Donnell *et al* 2016, Textor *et al* 2019) and is the main source of C used for GHG production in inland waters (Dean *et al* 2020). However, given

that we did not see significant differences in dissolved CO_2 concentrations among vegetation class types, the increased DOM export to ponds may not lead to increased GHG flux potentials in this landscape.

Thaw disturbance events that result in mass sediment movement (e.g. active layer detachments and retrogressive thaw slumps) are projected to increase in frequency with climate warming (Lewkowicz and Harris 2005, Lewkowicz and Way 2019). Our results suggest these events will cause localized decreases in DOC export to inland waters due to the removal of vegetation cover and/or increased sorption of DOM to mineral soils. While DOC export will decrease, our results also suggest there may be higher proportions of autochthonous DOM produced in ponds in the ALDs. The lack of significant differences in dissolved CO_2 concentrations suggest disturbance events, despite altering DOM export and composition, do not cause increased CO_2 flux potentials at the CBAWO. Given that the current assumption is permafrost thaw and disturbance events increase microbial activity and GHG fluxes, we propose additional research is necessary to constrain what physical, environmental, and/or biological factors determine whether or not thaw and disturbance events increase (Turetsky *et al* 2020), decrease (Serikova *et al* 2019), or do not significantly change (this study) GHG flux potentials from permafrost environments.

4.4. Conclusions

Combined, our findings suggest that the surrounding terrestrial landscape type largely determines the DOM characteristics of ponds in this High Arctic environment. An increase in the magnitude and frequency of both rainfall events and permafrost disturbances will alter DOC concentrations and DOM characteristics, but these changes may not necessarily translate into increasing GHG flux potentials from ponds. Despite geochemical measurements and DOM spectroscopy indicating DOM in ponds located in ALDs had more bio-labile characteristics and autochthonous DOM production than in ponds located in undisturbed regions, dissolved CO_2 concentrations were not significantly different between the two pond groups. We conclude that surrounding vegetation and hydrology are the major drivers of C cycling and DOM composition in small High Arctic ponds, with rainfall events affecting signatures of allochthonous DOM and potentially importing DOM into ponds from the surrounding landscape.

Data availability statement

All data associated with this study will be posted on the Polar Data Catalogue data repository (www.polardata.ca).

The data that support the findings of this study are available upon reasonable request from the authors.

Acknowledgments


We thank: S Koziar for invaluable lab assistance, the 2018 CBAWO research team, Polar Continental Shelf Program (PSCP) for logistical support, C Beel for feedback on an earlier version of this manuscript, and the anonymous reviewers whose comments helped improve this manuscript. Funding for research at the CBAWO was provided by Arctic Net Network Centre of Excellence grants and individual NSERC Discovery Grants to SFL and MJL. JKH received additional support from a Robert Gilbert Postdoctoral Fellowship awarded by the Department of Geography and Planning at Queen's University. JKYH and FMC received additional funding from NSTP (Polar Knowledge Canada). Research at the CBAWO has been carried out with the permission and support of the Hamlet of Resolute.

ORCID iDs

J K Heslop  <https://orcid.org/0000-0002-8243-4456>

J K Y Hung  <https://orcid.org/0000-0001-5245-0896>

H Tong  <https://orcid.org/0000-0001-9848-3378>

M J Lafrenière  <https://orcid.org/0000-0002-9639-6825>

References

- Abbott B *et al* 2014 Elevated dissolved organic carbon biodegradability from thawing and collapsing permafrost *J. Geophys. Res. Biogeosci.* **119** 2049–63
- Beel C R *et al* 2018 Fluvial response to a period of hydrometeorological change and landscape disturbance in the Canadian High Arctic *Geophys. Res. Lett.* **45** 10446–55
- Beel C R, Lamoureux S F, Orwin J F, Pope M A, Lafrenière M J and Scott N A 2020 Differential impact of thermal and physical permafrost disturbance on High Arctic dissolved and particulate fluvial fluxes *Sci. Rep.* **10** 11836
- Bintanja R and Andry O 2017 Towards a rain-dominated Arctic *Nat. Clim. Change* **7** 263–7
- Bogard M J, Kuhn C D, Johnston S E, Striegl R G, Holtgrieve G W, Dornblaser M M, Spencer R G M, Wickland K P and Butman D E 2019 Negligible cycling of terrestrial carbon in many lakes of the arid circumpolar landscape *Nat. Geosci.* **12** 180–5
- Bouchard F, Laurion I, Prékienis V, Fortier D, Xu X and Whittaker M J 2015 Modern to millennium-old greenhouse gases emitted from ponds and lakes of the Eastern Canadian Arctic (Bylot Island, Nunavut) *Biogeosciences* **12** 7279–98
- Cazzanelli M, Forsström L, Rautio M, Michelsen A and Christoffersen K S 2012 Benthic resources are the key to *Daphnia middendorffiana* survival in a High Arctic pond *Freshw. Biol.* **57** 541–51
- Coch C, Lamoureux S F, Knoblauch C, Eiseheid I, Fritz M, Obu J and Lantuit H 2018 Summer rainfall dissolved organic carbon, solute, and sediment fluxes in a small Arctic coastal catchment on Herschel Island (Yukon Territory, Canada) *Arct. Sci.* **4** 750–80
- Cory R M *et al* 2010 Effect of instrument-specific response on the analysis of fulvic acid fluorescence spectra *Limnol. Oceanogr. Methods* **8** 67–78
- Dean J F *et al* 2020 East Siberian Arctic inland waters emit mostly contemporary carbon *Nat. Commun.* **11** 1627
- Douglas P M J *et al* 2020 Clumped isotopes link older carbon substrates with slower rates of methanogenesis in northern lakes *Geophys. Res. Lett.* **47** e2019GL086756
- Downing B D *et al* 2009 Quantifying fluxes and characterizing compositional changes of dissolved organic matter in aquatic systems in situ using combined acoustic and optical measurements *Limnol. Oceanogr. Methods* **7** 119–31
- Edlund S A 1993 The distribution of plant communities on Melville Island, Arctic Canada. In Christie, RL, and McMillan, J (eds.): the geology of Melville Island, Arctic Canada *Geol. Surv. Can. Bull.* **450** 247–55
- Edwards R and Treitz P 2018 Vegetation greening trends at two sites in the Canadian Arctic: 1984–2015 *Arct. Antarct. Alpine Res.* **49** 601–19
- Emmertson C A, St. Louis V L, Lehnherr I, Graydon J A, Kirk J L and Rondeau K J 2016 The importance of freshwater systems to the net atmospheric exchange of carbon dioxide and methane with a rapidly changing high Arctic watershed *Biogeosciences* **13** 5849–63
- Favaro E and Lamoureux S F 2015 Downstream patterns of suspended sediment transport in a High Arctic river influenced by permafrost disturbance and recent climate change *Geomorphology* **246** 359–69
- Fouché J, Lafrenière M J, Rutherford K and Lamoureux S 2017 Seasonal hydrology and permafrost disturbance impacts on dissolved organic matter composition in High Arctic headwater catchments *Arct. Sci.* **3** 378–405
- Frey K E, Sobczak W V, Mann P J and Holmes R M 2016 Optical properties and bioavailability of dissolved organic matter along a flow-path continuum from soil pore waters to the Kolyma River mainstem, East Siberia *Biogeosciences* **13** 2279–90
- Helms J R, Stubbins A, Ritchie J D, Minor E C, Kieber D J and Mopper K 2008 Absorption spectral slopes and slope ratios as indicators of molecular weight, source, and photobleaching of chromophoric dissolved organic matter *Limnol. Oceanogr.* **53** 955–69
- Huguet A, Vacher L, Relexans S, Saubusse S, Froidefond J M and Parlanti E 2009 Properties of fluorescent dissolved organic matter in the Gironde Estuary *Org. Geochem.* **40** 706–19
- Hung J K Y and Treitz P 2020 Environmental land-cover classification for integrated watershed studies: Cape Bounty, Melville Island, Nunavut *Arctic Sci. Early Version* **6** 404–22
- Judd K E and Kling G 2002 Production and export of dissolved C in arctic tundra mesocosms: the roles of vegetation and water flow *Biogeochemistry* **60** 213–34
- Kalbitz K, Schwesig D, Rethemeyer J and Matzner E 2005 Stabilization of dissolved organic matter by sorption to the mineral soil *Soil Biol. Biochem.* **37** 1319–31
- Kellerman A *et al* 2015 Persistence of dissolved organic matter in lakes related to its molecular characteristics *Nat. Geosci.* **8** 454–7
- Kling G W, Kipphut G W and Miller M C 1992 The flux of CO₂ and CH₄ from lakes and rivers in arctic Alaska *Hydrobiologia* **240** 23–36
- Kuhn M K, Lundin E J, Giesler R, Johansson M and Karlsson J 2018 Emissions from thaw ponds largely offset the carbon sink of northern permafrost wetlands *Sci. Rep.* **8** 9535
- Lafrenière M, Louiseize N L and Lamoureux S F 2017 Active layer slope disturbances affect seasonality and composition of dissolved nitrogen export from High Arctic headwater catchments *Arctic Sci.* **3** 429–50
- Lamhonwah D, Lafrenière M J, Lamoureux S F and Wolfe B B 2016 Multi-year impacts of permafrost disturbance and thermal perturbation on High Arctic stream chemistry *Arctic Sci.* **3** 254–76
- Lamoureux S F and Lafrenière M J 2018 More than just snowmelt: integrated watershed science for changing climate and permafrost at the Cape Bounty Arctic Watershed Observatory *WIREs Water* **5** e1255
- Laurion I, Vincent W F, Macintyre S, Retamal L, Dupont C, Francus P and Pienitz R 2010 Variability in greenhouse gas

- emissions from permafrost thaw ponds *Limnol. Oceanogr.* **55** 115–33
- Lewis T, Lafrenière M J and Lamoureux S F 2012 Hydrochemical and sedimentary responses of paired High Arctic watersheds to unusual climate and permafrost disturbance, Cape Bounty, Melville Island, Canada *Hydrol. Process.* **26** 2003–18
- Lewkowicz A G and Harris C 2005 Frequency and magnitude of active-layer detachment failures in discontinuous and continuous permafrost, northern Canada *Permafr. Periglac. Process.* **16** 115–30
- Lewkowicz A G and Way R 2019 Extremes of summer climate trigger thousands of thermokarst landslides in a High Arctic environment *Nat. Commun.* **10** 1329
- Littlefair C A, Tank S E and Kokelj S V 2017 Retrogressive thaw slumps temper dissolved organic carbon delivery to streams of the Peel Plateau, NWT, Canada *Biogeosciences* **14** 5487–505
- Mann P et al 2014 Evidence for key enzymatic controls on metabolism of Arctic river organic matter *Glob. Change Biol.* **20** 1089–100
- Mann P et al 2016 Pan-Arctic trends in terrestrial dissolved organic matter from optical measurements *Front. Earth Sci.* **4** 25
- Massicotte P, Stedmon C and Markager S 2017 Spectral signature of suspended fine particulate material on light absorption properties of CDOM *Mar. Chem.* **196** 98–106
- Mcfadden S 2019 Fine-scale ground surface vertical displacement and soil water processes in the Canadian High Arctic *MS Thesis* Queen's University
- Metcalfe D B et al 2018 Patchy field sampling biases understanding of climate change impacts across the Arctic *Nat. Ecol. Evol.* **2** 1443–8
- O'Donnell J et al 2016 DOM composition and transformation in boreal forest soils: the effects of temperature and organic-horizon decomposition state *J. Geophys. Res. Biogeosci.* **121** 2727–44
- Ohno T 2002 Fluorescence inner-filtering correction for determining the humification index of dissolved organic matter *Environ. Sci. Technol.* **36** 742–6
- Pickard A et al 2017 Temporal changes in photoreactivity of dissolved organic carbon and implications for aquatic carbon fluxes from peatlands *Biogeosciences* **14** 1793–809
- Polishchuk Y M, Bogdanov A N, Muratov I N, Polishchuk V Y, Lim A, Manasypov R M, Shirokova L S and Pokrovsky O S 2018 Minor contribution of small thaw ponds to the pools of carbon and methane in the inland waters of the permafrost-affected part of the Western Siberian Lowland *Environ. Res. Lett.* **13** 045002
- Poulin B A, Ryan J N and Aiken G R 2014 Effects of iron on optical properties of dissolved organic matter *Environ. Sci. Technol.* **48** 10098–106
- Rutledge S et al 2010 Photodegradation leads to increased carbon dioxide losses from terrestrial organic matter *Glob. Change Biol.* **16** 3065–74
- Schuur E et al 2015 Climate change and the permafrost carbon feedback *Nature* **520** 171–9
- Serikova S, Pokrovsky O S, Laudon H, Krickov I V, Lim A G, Manasypov R M and Karlsson J 2019 High carbon emissions from thermokarst lakes of Western Siberia *Nat. Commun.* **10** 1552
- Spencer R G M, Aiken G R, Dyda R Y, Butler K D, Bergamaschi B A and Hernes P J 2010 Comparison of XAD with other dissolved lignin isolation techniques and a compilation of analytical improvements for the analysis of lignin in aquatic settings *Org. Geochem.* **41** 445–53
- Spencer R G M, Butler K D and Aiken G R 2012 Dissolved organic carbon and chromophoric dissolved organic matter properties of rivers in the USA *J. Geophys. Res. Biogeosci.* **117** G03001
- Spencer R G M, Mann P J, Dittmar T, Eglinton T I, McIntyre C, Holmes R M, Zimov N and Stubbins A 2015 Detecting the signature of permafrost thaw in Arctic rivers *Geophys. Res. Lett.* **42** 2830–5
- Strauss J et al 2017 Deep Yedoma permafrost: a synthesis of depositional characteristics and carbon vulnerability *Earth Sci. Rev.* **172** 75–86
- Tank S et al 2020 Landscape matters: predicting the biogeochemical effects of permafrost thaw on aquatic networks with a state factor approach *Permafr. Periglac. Process.* **31** 358–70
- Textor S, Wickland K P, Podgorski D C, Johnston S E and Spencer R G M 2019 Dissolved organic carbon turnover in permafrost-influenced watersheds of interior Alaska: molecular insights and the priming effect *Front. Earth Sci.* **7** 275
- Thiel G 2018 Investigating dissolved organic matter cycling in High Arctic ponds and soils *MS Thesis*, Queen's University
- Toohey R C, Herman-Mercer N M, Schuster P F, Mutter E A and Koch J C 2016 Multidecadal increases in the Yukon River Basin of chemical fluxes as indicators of changing flowpaths, groundwater, and permafrost *Geophys. Res. Lett.* **43** 2016GL070817
- Turetsky M R et al 2020 Carbon release through abrupt permafrost thaw *Nat. Geosci.* **13** 138–43
- Vonk J E et al 2013 High biolability of ancient permafrost carbon upon thaw *Geophys. Res. Lett.* **40** 2689–93
- Vonk J E et al 2015 Reviews and syntheses: effects of permafrost thaw on Arctic aquatic ecosystems *Biogeosciences* **12** 7129–67
- Walter Anthony K M et al 2014 A shift of thermokarst lakes from carbon sources to sinks during the Holocene epoch *Nature* **511** 452–6
- Walter K M et al 2006 Methane bubbling from Siberian thaw lakes as a positive feedback to climate warming *Nature* **443** 71–75
- Wang J, Lafrenière M J, Lamoureux S F, Simpson A J, Gélinas Y and Simpson M J 2018 Differences in riverine and pond water dissolved organic matter composition and sources in Canadian High Arctic watersheds affected by active layer detachments *Environ. Sci. Technol.* **52** 1062–71
- Wauthy M et al 2020 Permafrost thaw stimulates primary producers but has a moderate effect on primary consumers in subarctic ponds *Ecosphere* **11** e03099
- Wauthy M, Rautio M, Christoffersen K S, Forsström L, Laurion I, Mariash H L, Peura S and Vincent W F 2018 Increasing dominance of terrigenous organic matter in circumpolar freshwaters due to permafrost thaw *Limnol. Oceanogr. Lett.* **3** 186–98
- Weishaar J L, Aiken G R, Bergamaschi B A, Fram M S, Fujii R and Mopper K 2003 Evaluation of specific ultraviolet absorbance as an indicator of the chemical composition and reactivity of dissolved organic carbon *Environ. Sci. Technol.* **37** 4702–8
- Wilson H F and Xenopoulos M A 2009 Effects of agricultural land use on the composition of fluvial dissolved organic matter *Nat. Geosci.* **2** 37–41
- Zolkos S, Tank S E and Kokelj S V 2018 Mineral weathering and the permafrost carbon-climate feedback *Geophys. Res. Lett.* **45** 9623–32